DOI: 10.1002/anie.201104104

Imaging Agents

Ultrasmall Rigid Particles as Multimodal Probes for Medical Applications

*François Lux, Anna Mignot, Pierre Mowat, Cédric Louis, Sandrine Dufort, Claire Bernhard, Franck Denat, Frédéric Boschetti, Claire Brunet, Rodolphe Antoine, Philippe Dugourd, Sophie Laurent, Luce Vander Elst, Robert Muller, Lucie Sancey, Véronique Josserand, Jean-Luc Coll, Vasile Stupar, Emmanuel Barbier, Chantal Rémy, Alexis Broisat, Catherine Ghezzi, Géraldine Le Duc, Stéphane Roux, Pascal Perriat,** and *Olivier Tillement*

Over the past two decades, nanoparticles have been developed in the field of theranostic[1,2] with the objective of meeting three requirements: 1) to exhibit long circulation in body fluids with major accumulation in tumour tissues due to their active or passive targeting properties (enhanced permeability and retention (EPR) effect);[3] 2) to be rapidly eliminated through the renal route to ensure a sufficient difference in concentration between healthy and diseased zones; 3) to display therapeutic potential and contrast properties.[4,5] This latter requirement was reinforced by the simultaneous development of devices combining imaging techniques, such as 1) high-sensitive X-ray tomography, positron emission tomography, or single-photon emission computed tomography and 2) magnetic resonance imaging (MRI) with high spatial resolution.[6,7]

However, it is still a great challenge to ensure both appropriate renal elimination (necessarily achieved using particles < 5.5 nm in size)[8] and multimodality (requiring molecules that systematically enlarge the particle size to a non-adequate extent). For instance, quantum dots[9] or gold clusters[10] do not exhibit both features as they require coatings that are too prohibitive in size to ensure multimodality. After reviewing the solutions proposed in scientific literature,[11–13] the most promising strategies rely on the elaboration of silica- or polymeric-based structures that incorporate different functional entities, such as dyes for fluorescence imaging, magnetic complexes for MRI, radioactive elements for scintigraphy or curie-therapy, heavy elements for interacting with X- or γ-rays, neutron absorbers for neutron-therapy or sensitizers for photodynamic therapy. Concerning multifunctional silica-based particles, even the most investigated technologies (i.e., Stöber or reverse emulsion methods) failed to yield objects smaller than 10 nm in size.

Here we propose an original top-down method consisting in the fragmentation of sub-10 nm structures already possessing all the desired functions (see Supporting Information). Briefly, these starting structures consist of core (gadolinium oxide)–shell (polysiloxane) particles developed by our group which offer several features and functionalities, but are too large in size to escape hepatic clearance.[14] Gadolinium was selected as contrast agent on account of its paramagnetic properties and because of its commercial use in approximately 45% of all MRI analyses.[15] The starting structures displayed an average core size of 3.5 nm and a shell thickness of 0.5 nm. The fluorophore-encapsulated shell was rendered functionally active by modified 1,4,7,10-tetraazacyclododecane-1,4,7,10-tetraacetic acid (DOTA) ligands which are able to chelate core gadolinium ions. In aqueous solutions, the

[*] Dr. A. Mignot, Prof. P. Perriat
Matériaux Ingénierie et Science, INSA-Lyon, UMR 5510 CNRS, Université de Lyon, 69621 Villeurbanne Cedex (France)
and
Campus LyonTech La Doua, INSA-Lyon, Bâtiment Blaise Pascal 7 avenue Jean Capelle, 69621 Villeurbanne cedex (France)
E-mail: Pascal.Perriat@insa-lyon.fr
Dr. F. Lux, Dr. A. Mignot, Dr. P. Mowat, Prof. O. Tillement
Laboratoire de Physico-Chimie des Matériaux Luminescents, UMR 5620 CNRS – Université Claude Bernard Lyon 1, Université de Lyon, 69622 Villeurbanne Cedex (France)
Dr. A. Mignot, Dr. C. Louis, Dr. S. Dufort
Nano-H SAS, 38070 Saint-Quentin Fallavier (France)
Dr. C. Bernhard, Prof. F. Denat
Institut de Chimie Moléculaire de l'Université de Bourgogne, UMR CNRS 5260, Université de Bourgogne, 21078 Dijon Cedex (France)
Dr. F. Boschetti
CheMatech, 21000 Dijon (France)
Dr. C. Brunet, Prof. R. Antoine, Prof. P. Dugourd
Laboratoire de Spectrométrie Ionique et Moléculaire, UMR CNRS 5579, Université Claude Bernard Lyon 1, 69622 Villeurbanne Cedex (France)
Dr. S. Laurent, Prof. L. V. Elst, Prof. R. Muller
Univ Mons, NMR & Mol Imaging Lab, Dept Gen Organ & Biomed Chem, B-7000 Mons (Belgium)
Dr. L. Sancey, Dr. V. Josserand, Prof. J.-L. Coll
INSERM, CRI, U823, Inst Albert Bonniot, 38042 Grenoble 9 (France)
Dr. V. Stupar, Dr. E. Barbier, Dr. C. Rémy
Université Grenoble 1, Grenoble Institut des Neurosciences, UMR S836, Grenoble (France)
Dr. V. Stupar, Dr. E. Barbier, Dr. C. Rémy
Inserm, U826, Grenoble (France)
Dr. A. Broisat, Prof. C. Ghezzi
Laboratoire radiopharmaceutique bioclinique, INSERM U877, Faculté de médecine de Grenoble, 38700 La Tronche (France)
Dr. G. Le Duc
European Synchrotron Radiation Facility, ID 17 Biomedical Beamline, BP220, 38043 Grenoble (France)
Prof. S. Roux
Institut UTINAM, UMR 6213 CNRS – Université de Franche-Comté, 25030 Besançon Cedex (France)

Supporting information for this article is available on the WWW under http://dx.doi.org/10.1002/anie.201104104.

ligands strongly accelerate the core dissolution leading to a hollow polysiloxane sphere. This latter collapses and fragments into small and rigid platforms (SRPs) of polysiloxane. These SRPs possess all the properties of the initial structure, bearing on their surface DOTA molecules that are partly chelated to dissolved gadolinium cations. DOTA was given preference over acyclic chelates, due to its higher complexation constant,[16] its lower kinetics that limit transmetallation with endogen cations such as Ca^{2+} and reduced toxicity for patients with severe renal dysfunction.[17,18] Our study aims to confirm the relevance of this strategy 1) by reporting the chemical and size characterization of the SRPs obtained as described above and 2) by demonstrating that they can be detected in vivo by four different techniques, namely fluorescence imaging, MRI, scintigraphy, and X-ray computed tomography.

Although the starting core–shell particles have an average size of only 4.5 ± 0.1 nm, owing to a mean standard deviation of 2 ± 0.2 nm, a significant number of these particles exhibit a size > 5.5 nm, resulting in undesirable hepatic clearance. In order to obtain SRPs without any residual Gd-oxide core, a sufficient amount of DOTA (at least two DOTA per Gd atom) had to be added. Moreover, the hydrodynamic size distribution of the SRPs obtained was entirely below 5.5 nm, with an average size of 3 ± 0.1 nm (see Supporting Information). Expectedly, the average size using fluorescence correlation spectroscopy was slightly larger (about 4 nm), as the particles measured by this technique are those that encapsulate the bulky organic Cy5.5 fluorophores. The molecular weight was estimated based on electrospray-mass spectrometry (Figure 1c) using a multiplicative correlation algorithm (see Supporting Information).[19] A mass of approximately 8.5 ± 1 kDa was obtained which resulted, after correlation with inductively coupled plasma mass spectrometry (ICP-MS) data, in a chemical formula of 10 DOTA, 7 Gd and 27 Si per particle. The scheme of a typical particle displaying this chemistry (Figure 1a) shows that it has effectively a size of around 3 nm (see Supporting Information for details). In addition, the respective proportions of free and metal chelating ligands were verified by means of luminescence dosages. ICP-MS analysis revealed that 30% of DOTA are free whereas luminescence experiments yielded a value of about 40%. This non-negligible proportion of free ligands (30–40%) appears to be useful for scintigraphic applications, as it enables the immobilization of numerous radioactive isotopes onto SRPs. It increases also the relaxation properties of SRPs through chelation of supplementary paramagnetic atom or provides them with therapeutic properties through binding to heavy elements.

Longitudinal relaxivities per gadolinium were measured at 310 K, ranging between 0.1 and 60 MHz, following SRPs dispersion in aqueous solutions of NaCl (0.9%). These features were found to be significantly higher compared to those related to DOTA(Gd) and DTPA(Gd), regardless of the frequency used (Figure 1b). At higher field strengths (7 T), the r_1 value was equal to $6.0\ mM^{-1}s^{-1}$, that is, about twice the value of DOTA(Gd), one of the most frequently used MRI contrast agent. This increase may certainly be accounted for by the greater inertia of the rigid structure supporting the gadolinium cations. Indeed, these structures have been shown to significantly slow down the rotation rate of the relaxing species, leading to similar r_1 increases at high frequency (e.g., heavy polymers or dendrimers containing Gd complexes).[7,20–22]

Imaging experiments have been performed in vivo on mice and rats using fluorescence imaging, MRI, X-ray computed tomography (CT) and single photon emission CT (SPECT) in order to validate the efficiency of SRPs as multimodal contrast agents, to demonstrate the absence of hepatic clearance, and to assess their appropriate biodistribution. For all imaging modalities, solutions containing $GdCl_3$ or $^{111}InCl_3$ with a high radiochemical purity ($\geq 95\%$) were added to SRPs in order to increase the relaxivity or confer radioactive properties through chelation with free DOTA. SRPs were tangentially filtrated so as to eliminate the excess of metal atoms, they were then purified on-column by HPLC in the case of radiolabeling and

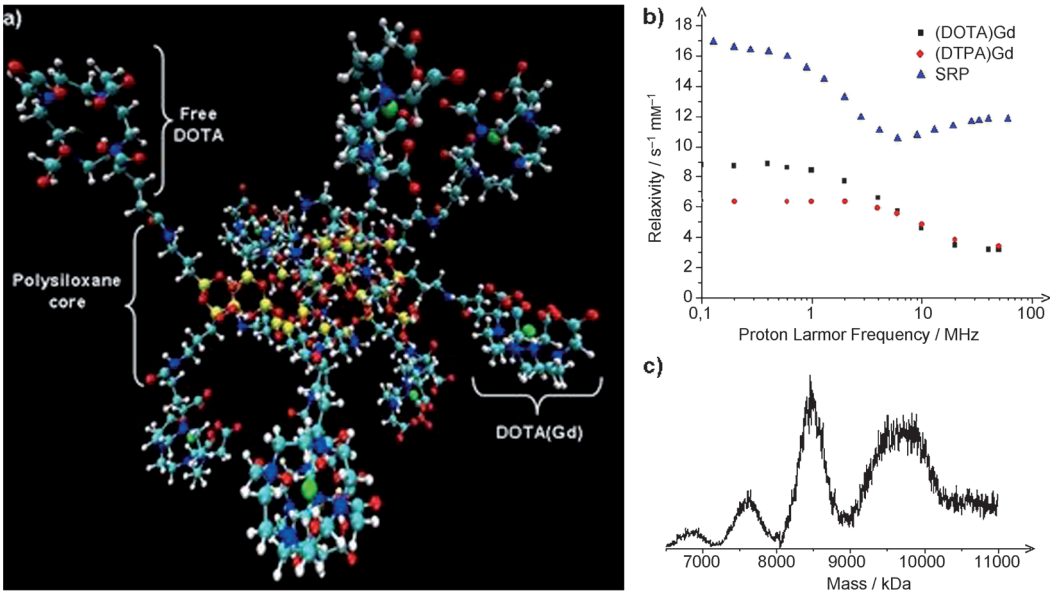

Figure 1. a) Representation of a typical SRP with a polysiloxane bone and DOTA(Gd) species grafted through amide functions (Si yellow, O red, C light blue, N blue, Gd green, H white). b) Proton NMRD data of SRPs (blue triangle), DOTA(Gd) (black squares), and DTPA(Gd) (red circles; DTPA = diethylenetriaminepentaacetic acid). Longitudinal relaxivities, r_1, are given per gadolinium. c) Mass spectrum calculated with a multiplicate correlation algorithm.

diluted in an aqueous solution composed of 145 mM NaCl and 10 mM HEPES at pH 7.4. SRPs used for fluorescence studies were doped by Cy5.5 during the sol–gel process (see Supporting Information for details). To better evaluate their contrast properties for fluorescence, injections (injected volume: 200 μL) were performed for three different particle concentrations given in mmol of gadolinium per liter of solution: 10 mM, 20 mM, and 40 mM. Fluorescence imaging was monitored over 24 h using three female swiss nude mice for various positions. In these experiments, SRPs were shown to only accumulate in kidneys and bladder (Figure 2). For all concentrations, no undesirable accumulation in lung and liver was detected, meaning that the particles are not recognized by the mononuclear phagocytic system and thus could undergo a prolonged vascular retention. Twenty-four hours after the injection, the mice were sacrificed, with fluorescence imaging of their organs confirming previous in vivo observations (Figure 2d). When performing MRI examinations at 7 T on 8-weeks-old male c57B1/6J mice, the same conclusions were drawn confirming the rapid clearance of SRPs by the renal route (Figure 3). Kidney visualization was evident 5 min after injection (injected volume: 80 μL at 40 mM in Gd) and that of bladder 25 min thereafter. On angiography images, brain blood vessels were highlighted, revealing rapid clearance from the blood stream. In comparison with DOTAREM (80 μL at 40 mM in Gd) administered under the same conditions or with the absence of a contrast agent, an undoubtedly better contrast was achieved. This may be accounted for by 1) the higher relaxivity of SRPs (twice that of DOTAREM) and 2) the greater residence time of particles compared to molecular compounds (see below for estimation of residence times). SPECT/CT imaging was performed on 8-weeks-old male c57B1/6J mice following injection through the tail vein (100 μL; 2.5 mM of gadolinium; 19.3 ± 2.2 MBq; colloidal stability over several days) (Figure 4). The counts were corrected for background and decay and expressed as a percentage of the injected dose (%ID). When mice were sacrificed 3 h following the injection, SRPs were, again,

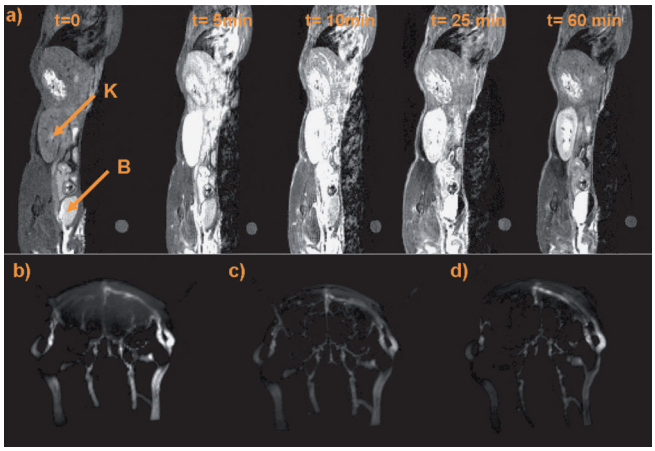

Figure 3. a) T_1-weighted images of a slice including one kidney (K) and the bladder (B) of a mouse before and after intravenous injection of SRPs. b–d) T_1-weighted images of the brain of a male c57Bl/6J mouse b) without contrast agent, c) with SRPs and d) with commercial DOTAREM at the same concentration of 40 mM.

detected in the kidneys and bladder (29.8 ± 6.8 %ID and 57.9 ± 27.4 %ID, respectively). For the other analyzed tissues, the uptake was lower than 0.2 %ID (or 1 %ID per gram), with no hepatic clearance being observed. In contrast, renal elimination occurred relatively fast since 12 min after injection, 25 % of the injected dose was detected in the bladder, with 50 % of the injected dose being detected at 74 min. Renal elimination was also highlighted by synchrotron radiation CT (SRCT) experiments performed at the biomedical beamline of the European Synchroton Radiation Facility (ESRF). In fact, 20 min after SRP injection in Fisher 344 rats (1.4 mL injected in saphena vein), the white coloration of both bladder and kidneys confirmed that the particles were present in these organs (Figure 5). Although the three other techniques were known to be more sensitive, we felt it important to verify that SRPs could be imaged by the same radiation used for therapy (indeed, SRPs are parts of the starting core–

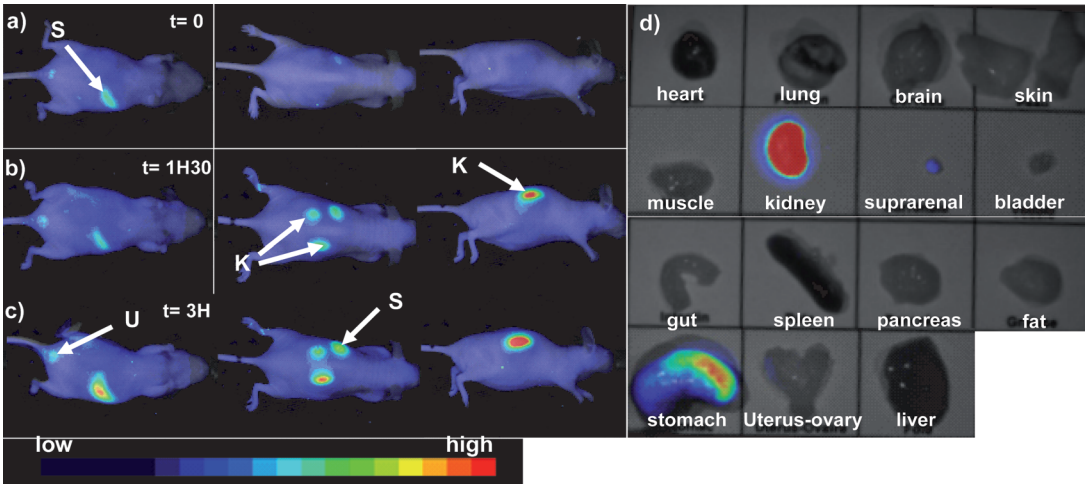

Figure 2. a–c) Fluorescence reflectance imaging of female swiss nude mice a) before, b) 90 min, and c) 3 h after SRP injection (concentration of 10 mM in Gd) (K: kidneys, S: stomach, U: urine). d) Fluorescence reflectance imaging of some organs after dissection of the nude mouse. Stomach fluorescence is due to mice alimentation.

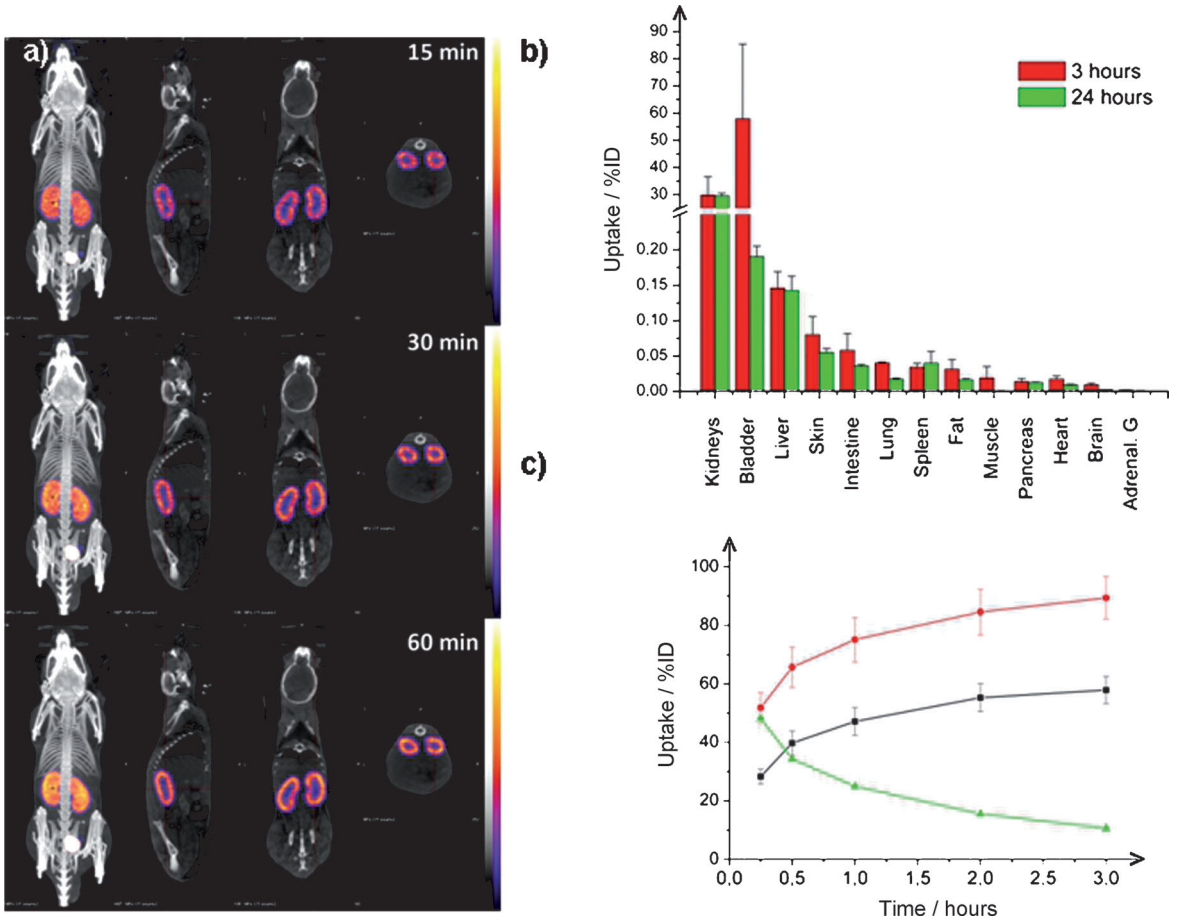

Figure 4. a) In vivo SPECT/CT imaging from 15 to 60 min after intravenous injection of SRPs on a male c57Bl/6J mouse. Left to right: Maximum intensity projection (MIP), sagittal, coronal, and transversal views centered on the right kidney. b) ^{111}In-SRP biodistribution at 3 h and 24 h p.i. (for the bladder, the uptake at 3 h corresponds to the bladder and the urine collected since the beginning of the experience, while at 24 h it corresponds to the bladder only). c) Black squares: ^{111}In-SRP accumulation in the bladder from 15 min to 3 h p.i. (average uptake on 8 animals); red circles: ^{111}In-SRP accumulation in the bladder and in the kidney from 15 min to 3 h p.i.; green triangles: remaining ID in the blood system from 15 min to 3 h p.i.

shell particles which were previously shown to be excellent in vitro[23] and in vivo[24] radiosensitizers on account of the high atomic number Z (64 for Gd) of ca. 20 wt.% of their components).

The performed experiments allow us to reasonably estimate SRPs' residence time, τ_{SRP}, within the blood stream. This estimate is based on the assumption that the amount of SRPs accumulated in an organ decreases according to the exponential law $e^{-t/\tau}$ where t is the time after injection and τ the residence time. According to MRI data (see fits in the Supporting Information) τ_{SRP} is equal to 13.2 min, being slightly higher (18 min) when using SPECT data (Figure 4*c*). This slight discrepancy can be explained by the fact that τ does not exactly reflect the same physical measurement when using both techniques (when using MRI, τ corresponds to particle disappearance from the heart while, when using SPECT, it refers to particle accumulation in the kidneys and bladder). Another point to mention is that, unlike Gd-chelates,[25] SRPs are cleared from the kidneys according to a multi-exponential law presenting a slow clearing component (see Figure 4c and similar figure in the Supporting Information). As a consequence, a significant proportion of SRPs can still be detected in the kidneys 24 h after their injection. Given this context, renal clearance is likely to depend on particle size with the larger particles circulating for a longer time than the smaller ones. This observation may account for the anomalous pharmacokinetic values found for the SRPs' residence times

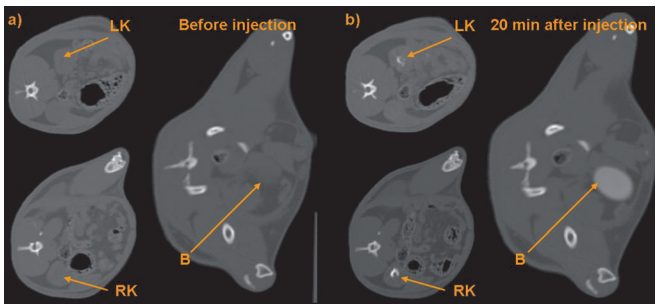

Figure 5. SRCT images of a series of successive transverse slices including the right and left kidneys (RK and LK, respectively) and the bladder (B) of a Fisher 344 rat. The images were recorded before and 20 min after the intravenous injection of SRPs.

compared to those of DOTAREM ($\tau_{SRP} = 13.2$ min versus $\tau_{DOTAREM} = 6.8$ min): due to their larger size, SRPs are restricted to the vascular compartment, whereas molecules may invade the extravascular space. The volume available being lower for particles, these latter are likely to undergo faster clearance than molecules. As the contrary is observed, interpretation of the data is only possible assuming that 1) renal clearance is lower for particles than for molecules and 2) renal clearance is inversely dependent on the particle size. This observation means that particles undergoing renal filtration are cleared more slowly when they are larger in size. This is an essential finding in the field of nanomedicine, highlighting the existence of an intermediate size range too large for efficient renal filtration but too small for hepatic clearance. As a great proportion of SRPs exhibit a long circulation time in the blood stream, these latter accumulate significantly in tumor tissues (data not shown here). These EPR effects[3] allow to achieve both a better contrast in imaging and an increased efficiency in therapy.

In conclusion, SRPs are new nanoparticle types, smaller than 5 nm in size, which are obtained by an original top-down process starting from a polysiloxane based core–shell structure, this latter being excreted in a still significant proportion by the hepatic route (feces). In contrast, the ultrasmall multifunctional silica-based particles (SRPs) present an unexpectedly long circulation in the blood stream and completely evade uptake by the reticulo-endothelial system. These SRPs can be additionally reinforced with rare-earth cations or radionuclides by further chelation of surface DOTA so as to enhance their contrast properties. Our results highlight that this new particles type enables animals imaging by using four different complementary techniques (MRI, fluorescence imaging, SPECT, CT). Compared to molecular compounds, SRPs' rigid structure allows for a substantial contrast enhancement in MRI studies and, more generally, longer and more detailed observations regardless of the imaging technique chosen. Lastly, as SRPs display a composition similar to that of the starting core–shells, they likely exhibit the same sensitizing properties and may, therefore, be considered as efficient therapeutic agents in different fields, such as neutron therapy and radiotherapy.

Received: June 15, 2011
Revised: September 12, 2011
Published online: November 4, 2011

Keywords: bioimaging · core–shell particles · gadolinium · imaging agents · theranostics

[1] C. Rivière, S. Roux, O. Tillement, C. Billotey, P. Perriat, *Ann. Chim. Sci. Mater.* **2006**, *31*, 351 – 357.
[2] B. Godin, J. H. Sakamoto, R. E. Serda, A. Grattoni, A. Bouamrani, M. Ferrari, *Trends Pharmacol. Sci.* **2010**, *31*, 199 – 205.
[3] M. Ferrari, *Nat. Rev.* **2005**, *5*, 161 – 171.
[4] M. Lewin, N. Carlesso, C. H. Tung, X. W. Tang, D. Cory, D. T. Scadden, R. Weissleder, *Nat. Biotechnol.* **2000**, *18*, 410 – 414.
[5] J. Kim, Y. Piao, T. Hyeon, *Chem. Soc. Rev.* **2009**, *38*, 372 – 390.
[6] A. Louie, *Chem. Rev.* **2010**, *110*, 3146 – 3195.
[7] A. E. Merbach, E. Toth, *The Chemistry of Contrast Agents in Medical Magnetic Resonance Imaging*, Wiley, New York, **2001**.
[8] H. S. Choi, W. Liu, K. Nasr, P. Misra, M. G. Bawendi, J. V. Frangioni, *Nat. Nanotechnol.* **2010**, *5*, 42 – 47.
[9] W. B. Cai, K. Chen, Z. B. Li, S. S. Gambhir, X. Y. Chen, *J. Nucl. Med.* **2007**, *48*, 1862 – 1870.
[10] C. Alric, J. Taleb, G. Le Duc, C. Mandon, C. Billotey, A. Le Meur-Herland, T. Brochard, F. Vocanson, M. Janier, P. Perriat, S. Roux, O. Tillement, *J. Am. Chem. Soc.* **2008**, *130*, 5908 – 5915.
[11] J. Xie, K. Chen, J. Huang, S. Lee, J. Whang, J. Gao, X. Li, X. Chen, *Biomaterials* **2010**, *31*, 3016 – 3022.
[12] W. J. Rieter, J. S. Kim, K. M. L. Taylor, H. An, W. Lin, T. Tarrant, W. Lin, *Angew. Chem.* **2007**, *119*, 3754 – 3756; *Angew. Chem. Int. Ed.* **2007**, *46*, 3680 – 3682.
[13] J.-L. Bridot, A.-C. Faure, S. Laurent, C. Rivière, C. Billotey, B. Hiba, M. Janier, V. Josserand, J.-L. Coll, L. Vander Elst, R. Müller, S. Roux, P. Perriat, O. Tillement, *J. Am. Chem. Soc.* **2007**, *129*, 5076 – 5084.
[14] D. Kryza, J. Taleb, M. Janier, L. Marmuse, I. Miladi, P. Bonazza, C. Louis, P. Perriat, S. Roux, O. Tillement, C. Billotey, *Bioconjugate Chem.* **2011**, *22*, 1145 – 1152.
[15] J. S. Ananta, B. Godin, R. Sehti, L. Moriggi, X. Liu, R. E. Serda, R. Krishnamurthy, R. D. Bolskar, L. Helm, M. Ferrari, L. J. Wilson, P. Decuzzi, *Nat. Nanotechnol.* **2010**, *5*, 815 – 821.
[16] K.-P. Eisenwiener, P. Powell, H. R. Mäcke, *Bioorg. Med. Chem. Lett.* **2000**, *10*, 2133 – 2135.
[17] H. S. Thomsen, *Eur. Radio.* **2006**, *16*, 2619 – 2621.
[18] C. Francès, P. Senet, D. Lipsker, *La Revue de Médecine Interne* **2011**, *32*, 358 – 362.
[19] J. J. Hagen, C. A. Monig, *Anal. Chem.* **1994**, *66*, 1877 – 1883.
[20] J. Henig, E. Toth, J. Hengelmann, S. Gottshalk, H. A. Mayer, *Inorg. Chem.* **2010**, *49*, 6124 – 6138.
[21] Ref. [15].
[22] P. Voisin, E. J. Riboit, S. Miraux, A.-K. Bouzier-Sore, J.-F. Lahitte, V. Bouchaud, S. Mornet, E. Thiaudière, J.-M. Franconi, L. Raison, C. Labrugère, M.-H. Delville, *Bioconjugate Chem.* **2007**, *18*, 1053 – 1063.
[23] P. Mowat, A. Mignot, W. Rima, F. Lux, O. Tillement, C. Roulin, M. Dutreix, D. Bechet, S. Huget, L. Humbert, M. Barberi-Heyob, M. T. Aloy, E. Armandy, C. Rodriguez-Lafrasse, G. Le Duc, S. Roux, P. Perriat, *J. Nanosci. Nanotechnol.* **2011**, *11*, 1 – 7.
[24] S. Roux, O. Tillement, C. Billotey, J. L. Coll, G. Le Duc, C. Marquette, P. Perriat, *Int. J. Nanotechnol.* **2010**, *7*, 781 – 801.
[25] M. F. Tweedle, P. Wedeking, K. Kumar, *Invest. Radiol.* **1995**, *30*, 372 – 380.

